

User Level Integrity Monitoring and Quality Control for High Accuracy Positioning using GPS/INS Measurements

Washington Y. Ochieng and Shaojun Feng

*Centre for Transport Studies, Department of Civil and Environmental Engineering
Imperial College London, London SW7 2AZ, United Kingdom*

Terry Moore, Chris Hill

IESSG, University of Nottingham, Nottingham NG7 2RD, United Kingdom

Chris Hide

Geospatial Research Centre, Private Bag 4800, Christchurch 8140, New Zealand

Abstract

This paper presents research undertaken to develop sensor level autonomous integrity monitoring and quality control to support centimetre level positioning in all conditions and environments as conceived under the SPACE (Seamless Positioning in All Conditions and Environments) project. The basic philosophy for integrity monitoring and quality control is early detection of anomalies which requires monitoring of the entire processing chain.

A number of novel concepts and algorithms are developed including algorithms to deal with special issues associated with carrier phase based integrity monitoring (including integration with INS), a new “difference test” integrity monitoring algorithm for detection of slowly growing errors, and a new group separation concept for simultaneous multiple failure exclusion.

Both real and simulated data are used to test the new algorithms. The results show that the new algorithms, when used together with selected existing ones, provide effective integrity monitoring and quality control for centimetre level seamless positioning in all conditions and environments.

Keywords: RAIM, Difference Test, Group Separation

1. Introduction

Integrity is a measure of the level of confidence in the accuracy of the positioning information supplied by a navigation system. It is vital for liability and safety critical applications such as air navigation and some

Location Based Services (LBS). GNSS integrity can be monitored at system level, user sensor level or both. User sensor level integrity monitoring falls under the category of Autonomous Integrity Monitoring (AIM) with a pure stand-alone approach referred to as the Receiver Autonomous Integrity Monitoring (RAIM). When a stand-alone GNSS system is aided by another sensor on the user platform, the monitoring process is commonly referred to as User Autonomous Integrity Monitoring (UAIM).

To date significant research effort has been directed at the development of algorithms and techniques for RAIM based on code phase (pseudorange) measurements. There has also been research to develop variations to RAIM particularly in the cases of sensor integration (Lee et al., 1999). The various RAIM algorithms in the literature are largely the same in principle with the differences mainly being in the selection of test statistics and thresholds (Brown, 1992, 1998).

Although positioning data from pseudorange measurements are suitable for many applications, carrier phase measurements are required for applications that require higher accuracy (at the decimetre level or better). Hence, an equivalent to Pseudorange RAIM (PRAIM) is required for carrier phase based positioning. This is referred to in this paper as Carrier RAIM (CRAIM). Pervan (1998) extended the PRAIM concept to CRAIM by assuming knowledge of integer ambiguities. However, this assumption is not always practical. Other approaches, e.g. by Michalson (1995), Pervan (1996, 2003) and Chang (2001) consider ambiguities as unknown variants

in the positioning equations. These methods generate float ambiguities with no attempt to fixing the integer values. Therefore, these methods could be unreliable due to the uncertainty in the ambiguity values. Chang (2001) developed a single difference based CRAIN approach which avoids strong correlation issues of the double differenced observable. Due to the same problem of float ambiguities above and the vulnerability of the single difference to receiver clock drift, this approach could also be unreliable.

Beyond the use the exclusive of the traditional measurements from GNSS (e.g. GPS), further complications arise when GNSS data is combined with data from other sensors (e.g. the INS). For example, most of the existing algorithms for monitoring the integrity of integrated GPS and INS sensors are based on the assumption that the INS provides valid (fault-free) data over short periods (Brown, 2006; Gold, 2004; Lee, 1999; Diesel, 1995). Therefore, the purpose of the GPS/INS integrity algorithm design is to detect and exclude any out of tolerance GNSS faults before correcting the INS. This is to prevent corrupted GNSS data from propagating back into GNSS/INS solution (Gold, 2004). The approach provides the integrity monitoring only for GNSS to guarantee the quality of updates provided to the integrated navigation Kalman filter. However, in reality the INS fails and thus to monitor the integrity of integrated GNSS/INS systems, failures in both GNSS and INS should be detected and excluded. Offer (2006) proposed a qualitative detection method which deals only with outliers, for example, in terms of repeated measurements being outside the sensor's dynamic range, and inertial sensor biases being outside the expected magnitudes.

In addition to the algorithmic weaknesses identified above, there are a number of challenges in the development of user requirements, Failure Modes and Effects Analysis (FMEA), conceptual and theoretical issues, and development of new algorithms. The challenges in development of user requirements include consolidation of services and potential environments, quantification of requirements in terms of performance parameters, and flexibility to carry out sensitivity analysis for detailed performance characterisation. The challenges in FMEA process include the analysis of characteristics, classification and modelling of potential failure modes, identification of common mode failures and 'difficult' failure modes, and FMEA for different system architectures and different data types. The challenges in theoretic issues include justification of assumptions such as error sources being independent and normally distributed, appropriate processing of data correlation and systems coupling. Once potential failure models are specified, the next step is to assess the capability of

existing algorithms against the failures, with the aim of identifying any 'difficult' failures. New algorithms are the developed to deal with any 'difficult' failures.

For the development of CRAIN, one of the difficulties is the common processing approach that uses the double differenced observable to eliminate the influence of common errors and mitigate the effect of those that exhibit a degree of spatial correlation. Related issues also include ambiguity resolution and validation; cycle slip detection and repair; potential failures associated with differencing (e.g. problems with the reference satellite used for differencing); potential simultaneous multiple failures (e.g. due to multipath and incorrect ambiguity resolution) and correlation of errors.

The results of the FMEA process above identified errors that grow slowly over time such as clock drift (referred to in this paper as Slowly Growing Errors or SGEs) and simultaneous multiple failures as being the most difficult to detect and exclude. This paper proposes a new algorithm based on the "difference test" concept for the former and a new approach based on group separation for the latter. Furthermore, CRAIN algorithms for both stand alone GPS and integrated GPS/INS systems are developed in the paper. These are presented in subsequent sections below.

2. Methodology

2.1 Difference Test

SGEs are of particular concern in filtering based UAIM because the Kalman filter tends to adapt to them. This results in the positioning solution being contaminated with the consequence of misleading information both in terms of accuracy and integrity. For this reason, early detection of this type of failure is vital. Failure detection in RAIM is based on statistical consistency checks using redundant measurements. There are two different RAIM schemes for use with measurements; snapshot and filtering (Brown, 1996). In the snapshot scheme only the current redundant measurements are used to check measurement consistency. However, in the filtering scheme current and previous measurements are used. In either case, the failure detection algorithms are based on a number of assumptions, the most important of which is that residual errors in the measurements are normally distributed. Failure detection consists of three main steps: the construction of a test statistic; the characterisation of the test statistic and the determination of a threshold to reflect the user requirement (e.g. probability of false alert); and decision making. One of the key features in the design of any integrity algorithm is its sensitivity to various types of failure modes. Unfortunately, neither the snapshot nor filtering methods are designed for detecting SGEs. Current approaches for the detection of SGEs have

been shown to have significant weaknesses (Feng and Ochieng, 2007a). Therefore, a new algorithm is needed to deal with SGEs.

Normally GPS exhibits long term stability with normal residual measurement noise. However, in the presence of SGEs, the GPS residuals exhibit a rate of growth. Therefore, a test statistic constructed to reflect whether there is a significant difference between the current residuals and residuals a certain time period ago has the potential to enable the detection of SGEs. The ratio test which is based on the F distribution is normally used to test whether there is a significant difference between two independent variants. Hence, the ratio test may be applicable in comparing a faulty variant with fault-free variant. However, if a ramp error occurs before the test, the ratio test cannot give the correct decision. For a ramp error, the ratio over a fixed time interval converges to one with the increase in time, which gives misleading information. Therefore, a new test based on the difference between the conventional test statistics at different epochs is referred to in this paper as the “difference test”.

The new test statistic is expressed as:

$$T_{\Delta t} = \sqrt{SSE_t} - \sqrt{SSE_{t-\Delta t}} \quad (1)$$

Where, t is current time and Δt is the time interval selected. The corresponding degrees of freedom are denoted as dof_2 and dof_1 respectively.

The test statistic is actually based on a moving window and thus always captures the difference between the two edges of the window.

Clearly, it is imperative to characterise and describe the distribution of the new test statistic. This relatively complex task must be undertaken, for example, to enable the computation of the threshold. The norm of the conventional residual follows a Chi-distribution. Therefore, the test statistic ($T_{\Delta t}$) is in fact the difference of two Chi-distributed variants. Based on the analysis of the difference between mean (μ), standard deviation (σ), skewness (γ_1), kurtosis (γ_2) of two Chi-distributed variants, and simulation, it can be shown that a normal distribution $N(\mu_D, 1)$ over-bounds the test statistic ($T_{\Delta t}$). The mean of the normal distribution is expressed as:

$$\mu_D = \mu_d - \gamma_{1d} \quad (2)$$

Where μ_d is the theoretical mean of the difference of two Chi-distributed variants, $\gamma_{1d} = ((\gamma_{12})^{\frac{1}{3}} - (\gamma_{11})^{\frac{1}{3}})\sigma_d / 2$ is the conservative offset factor with γ_{12} and γ_{11} being the skewness corresponding to dof_2 and dof_1 respectively, and σ_d is the theoretical standard deviation of the difference of two Chi-distributed variants (Feng and Ochieng, 2007a).

Based on the above characterisation of the test statistic ($T_{\Delta t}$) in the “difference test”, A decision threshold can then be determined from the normal distribution $N(\mu_D, 1)$ by taking account of the required navigation performance (RNP), specifically, the integrity and continuity risk from which the probability of missed detection (P_{MD}) and the probability of false alert (P_{FA}) can be derived.

One important factor in the test statistic constructed in expression (1) is the time interval Δt . The choice of time interval depends on the rate of error growth and the length of the data buffer designed. The slower the error growth rate, the longer the time interval required to detect the error. To detect and identify the rate of SGEs, a multiple window scheme can be used at different time intervals. A comparison of performances of the *difference* and *conventional* test algorithms is undertaken and the results presented in the section on ‘field trials and results’.

2.2 CRAIM for GPS

Integrity monitoring algorithms are always coupled with positioning algorithms. The resolution of integer ambiguities is a prerequisite to the achievement of centimetre level positioning using carrier phase measurements from GNSS. If integer ambiguities are resolved correctly, then the CRAIM algorithms are a direct extension of PRAIM. Therefore, the resolution of integer ambiguities is a major issue in CRAIM.

In Kalman filtering based positioning, although not specifically a Kalman filtering task, ambiguity resolution is included within the filter used in this paper, rather than considering it as separate task. This is because tasks such as rearranging the double differenced ambiguity states when the reference satellite changes, removing ambiguity states when they are fixed and updating states with the fixed values are all necessary, and would require additional interfaces to the filter. The LAMBDA algorithm (De Jonge et al, 1996) is used to decorrelate the ambiguities to make the integer ambiguity search more efficient. Ambiguity validation is currently achieved

using the ratio test (Teunissen, 2005). Once the ambiguities have been resolved, it is necessary to remove the ambiguity states from the state vector of the Kalman filter, as well as to update the remaining states with the resolved integer values. If dual or triple frequencies are used, a cascaded approach is adopted for the resolution of ambiguities, starting with the long wavelength (e.g. wide-lane) measurements which have ambiguities that are readily resolved, and then moving to shorter wavelengths.

A combination of pseudorange, wide-lane and L1 carrier phase observables is used for the positioning. The pseudorange is the most robust but noisy, and can constrain the position solution to a certain level of accuracy. The wide-lane has a much longer wavelength (e.g. about 86 cm for L1-L2) than that of any single frequency carrier. Based on the constraint of the pseudorange solution, it is not difficult to meet the error budget for the wide-lane ambiguity resolution. A more accurate solution can then be determined based on the wide-lane. The better positioning solution enables the L1 ambiguity to be resolved more reliably. Hence, the accuracy of the final positioning solution is effectively determined by the L1 carrier phase measurements.

Although the innovation sequence in a Kalman filter contains information obtained from the previous states, it provides the most relevant source of information for integrity monitoring. It is similar to the residual in the snapshot RAIM method (Lee et al., 1999). However, when the double differenced measurements are used, the property of independence in the measurement noise properties is lost. However, this dependence is a mathematical correlation rather than a physical correlation. The measurement noise and covariance matrices in the Kalman filter are used to account for the correlation.

The proposed CRAIM algorithm employs four tests statistics, a full set and three subsets (formed based on the type of measurements i.e. pseudorange subset, wide-lane subset and L1 subset). These subset test statistics help to identify anomalies either in the L1, or L2 data.

The protection level can be determined using relevant information from the Kalman filter. One way is to use the position estimate uncertainty; the other way is to project the test statistic to the position error.

The elements of the covariance matrix (P) indicate the uncertainty of the state. The first three elements in the state are the position in North-East-Down (NED) coordinates. Therefore, $\sigma_H = \sqrt{P_{11} + P_{22}}$ indicates the horizontal position uncertainty. The position estimate uncertainty based horizontal protection level can be expressed as:

$$HPL_1 = k_H \sigma_H \quad (3)$$

where k_H is the factor that reflect the probability of missed detection which is derived from the integrity risk.

Another way to determine the protection level is to project the test statistic to the position error. A ratio of the position error to the test statistic, referred to as *SLOPE* can be calculated based on the observation matrix of Kalman filter. The method is similar to the conventional RAIM. The projection based horizontal protection level is denoted as HPL_2

To be conservative, the protection levels are determined by

$$HPL = \max(HPL_1, HPL_2) \quad (4)$$

Real data contaminated by simulated cycle slips are used to verify the performance of the algorithm. The details are given in the results section.

2.3 CRAIM for GPS/INS Integration

The GPS/INS integration is based on the Kalman filter as well. However, in addition to adding the inertial sensor error models in the state of the Kalman filter, the input observations to the Kalman filter are the differences between GPS based measurements and INS based predicted measurements. The carrier phase based RAIM for the integrated system is referred to in this paper as CUAIM (Carrier User Autonomous Integrity Monitoring). The construction of the test statistic, the calculation of corresponding threshold, and the determination of protection levels are the same as for the CRAIM algorithm for stand alone GPS.

Figure 1 shows the quality control process for a tightly coupled integrated GPS/INS architecture (Feng et al., 2007b). Both GPS and IMU data are sent to the pre-processing module for data screening. This is followed by a pseudorange based GPS RAIM to detect and exclude potential failures. The reason PRAIM is used separately is because the pseudorange measurement is robust. Furthermore, undetected pseudorange anomalies have a negative impact on carrier phase based positioning. In the PRAIM, the carrier phase measurement is excluded if the pseudorange measurement from the same satellites is excluded. Therefore, only the carrier phase measurements with corresponding acceptable pseudorange measurements are passed on to the CRAIM module. The CUAIM uses the measurements that have passed several tests. This is quality control process facilitates failure detection in either GPS, INS or both.

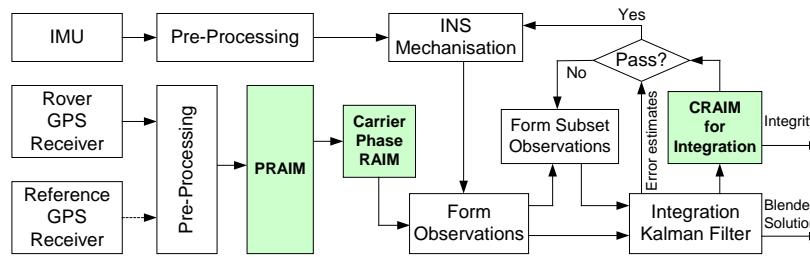


Fig. 1 The integrity monitoring for GPS/INS integration

2.4 Group Separation

Existing RAIM algorithms assume that only one satellite can have a significant error at a time. This assumption is reasonable for some applications such as en-route, terminal and Non-Precision Approach (NPA) phases of flight because the probability of a fault causing a ranging error large enough to cause the position error to exceed the alert limit (e.g. 556m for NPA (or even larger for en route and terminal navigation) is very low (Lee, 2004).

However, at the user level the satellite navigation system is not the only potential source of failure. Failures induced by the operational environment which have the potential to affect several measurements simultaneously have a higher probability of occurrence than satellite (system) related failures. In any case, the one failure assumption of current algorithms does not hold for applications with very stringent requirements such as aircraft landing. For such applications, it is crucial that simultaneous multiple failures are taken into account. Current methods that extend single failure detection and exclusion to cope with the multiple failures still rely on the assumption of one failure at a time even for a subset. In this case, the failure identification scheme removes one satellite at a time from the full set (all n measurements are used) and forms n first level subsets each consisting of $(n-1)$ measurements. If the failure has not been identified from the first level subset, one satellite will be removed from each first level subset each time to form a bank of second level subsets. Each second level subset consists of $(n-2)$ measurements. This process continues until multiple failures are detected and excluded or fails due to either a violation of the minimum required number of measurements, weak geometry or both.

Simultaneous multiple failures are generally of two types. In the first type, independent failures occur at the same time, each causing its corresponding ranging error to become unusually large. In the second type, multiple failures are affected by a common fault (correlated failures) that results in their respective ranging errors becoming unusually large. For the first type of multiple failures, the probability of occurrence is relatively low. Data snooping is probably the only effective way of

dealing with these failures. Simultaneous multiple failures are more likely to be of the second type. Therefore, potential common failure modes identified using prior-knowledge of GNSS and the user receiver measurements can be used to determine potential failure ‘groups’. The group most likely to fail has the highest priority for separation (exclusion) (Feng and Ochieng, 2006). This approach is referred to in this paper as the group separation method. For example, measurements may be grouped according to 1) navigation system; 2) satellites tracked by the same monitoring station; 3) the age of satellite; 4) satellite clock type; 5) the age of satellite clock; 6) satellite fault/event history; 7) elevation angle; 8) azimuth angle; 9) signal frequency; 10) signal to noise ratio.

3. Field trial and Results

Field trial data combined with simulated inertial sensor anomalies were used to demonstrate the performance of some of the algorithms proposed in this paper: the difference test method, carrier phase based RAIM for stand alone GPS, and carrier phase based RAIM for integrated GPS/INS systems.

The reference GPS receiver used is the Lecia SR530 geodetic RTK receiver which was set to output the pseudoranges (C1, P2) and carrier phase measurements (L1, L2) in the RINEX format. The rover GPS receiver used was the NovAtel OEM4 which was set to output the pseudoranges (C1, P2) and carrier phase measurements (L1, L2) in the RINEX format as well. The Inertial Measurement Unit (IMU) used was the Honeywell’s CIMU (Hide *et al*, 2006). The Rover receiver and IMU were mounted on the top of a car.

The trial was carried out on the runway of the Aberporth airport in the UK. The trial route and the position of the reference station are shown in Figure 2. The various equipments on the car were operated in static mode at the start for about 25 minutes. The car was then driven at different speeds along the runway.

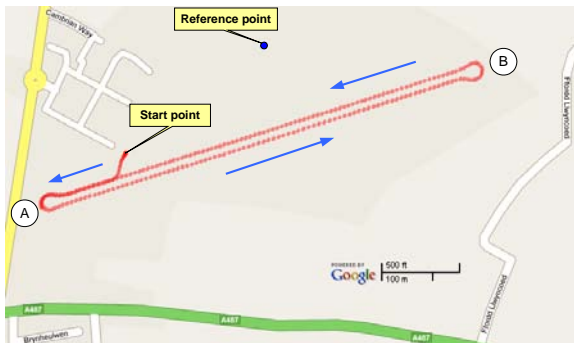


Fig. 2 Trial route (displayed using Google map API licensed for non-commercial use)

3.1 Results of difference test algorithm

Trial data (pseudorange measurements) contaminated by a simulated slowly growing error are used to verify the proposed methods below.

To demonstrate the performance of the algorithms, different time intervals for the “difference test” and different ramp errors start to apply on PRN 21 at the 1500th second from epoch 0. The required probability of false alert is $3.33 \times 10^{-7} / \text{sample}$ (RTCA/DO-229C, 2001). Figure 3 shows the test statistic (difference test) at a time interval of 360 seconds for a ramp error of 0.2m/s. The conventional test statistic is also shown in the figure. The thresholds for the “difference test” are the same as the differences in the number of visible satellites are the same, and vice versa. The comparison of the conventional and the difference test methods shows that the latter is able to detect the failure significantly earlier (by about 20 seconds) than the former.

Figure 4 shows the test statistic (difference test) at time intervals of 120, 240, and 360 seconds for a ramp error of 0.2m/s. It compares the conventional method with the difference test implementing a new early detection

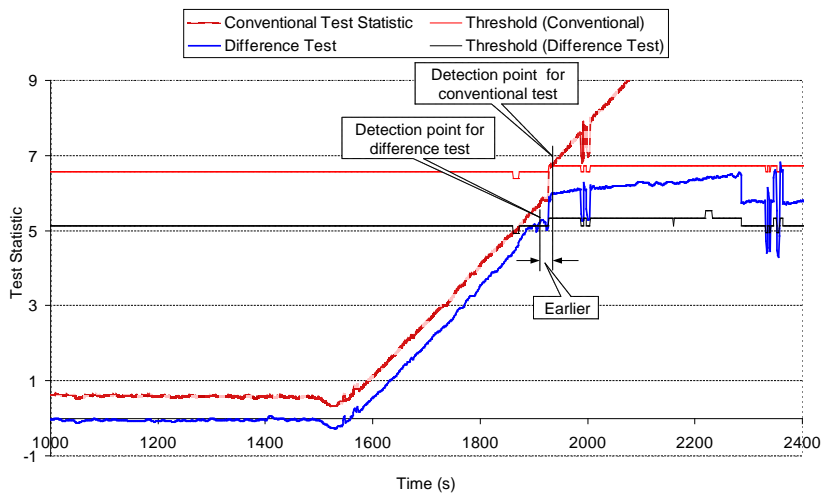


Fig. 3 Comparison of the conventional method and the difference test

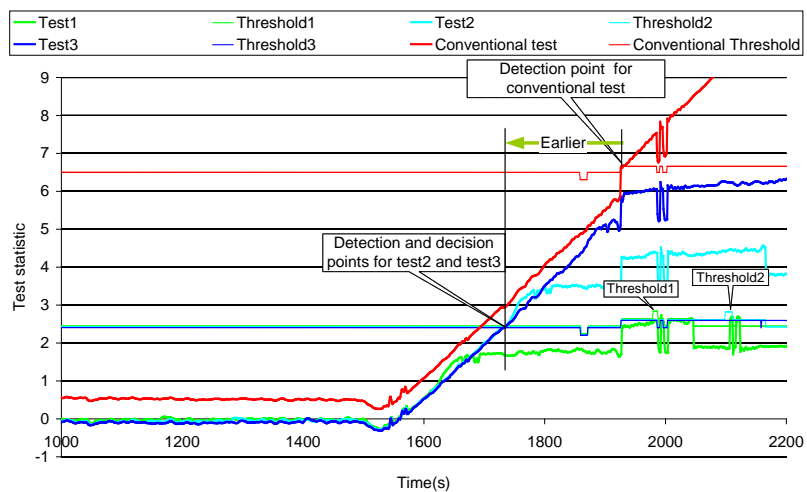


Fig. 4 Comparison of the conventional method and the difference test with the early detection scheme

scheme involving applying the difference test to a number of sequential epochs (Feng and Ochieng, 2007a). The algorithm with the shortest time interval (120s) is not sensitive to this error (test1 in the figure). While the algorithm with the longer time intervals (i.e. 240s and 360s) is sensitive to this error (test2 and test3 in the figure), and can detect the failure much earlier (about 180s) than the conventional method.

This difference test can be used to detect a failure significantly earlier compared to the conventional methods. Results demonstrate that it is able to detect a SGE about 20 seconds earlier than conventional method as shown in Figure 3. This is crucial for safety critical applications such as aviation where the time-to-alert ranges from 5 minutes for the En-route phase of flight to 6 seconds for Category I precision approach with even more stringent requirements expected for Category II and III precision approach (ICAO, 2006). The test statistics based on various time intervals can also be used to identify the rate of growth of error to support FMEA.

3.2 Results of GPS CRAIM Algorithm

Real data combined with simulated cycle slips are used to verify the performance of the CRAIM algorithm proposed in this paper. Based on the assumption that the cycle slips evade the detection in the pre-processing algorithms, the scenario that cycle slip events occur on two L2 carriers at the 200th second is demonstrated. Note that each event involves one cycle slip. The case where the cycle slip occurs on the reference satellite is equivalent to the use of a wrong set of ambiguities. It causes a jump in the test statistics and can be easily detected.

The reference satellite used in the computation of the differences changes at the 785th second in the positioning process. Under each scenario, the test statistic and the corresponding threshold of the full set and subsets are investigated. Figures 5 and 6 show the results of this scenario.

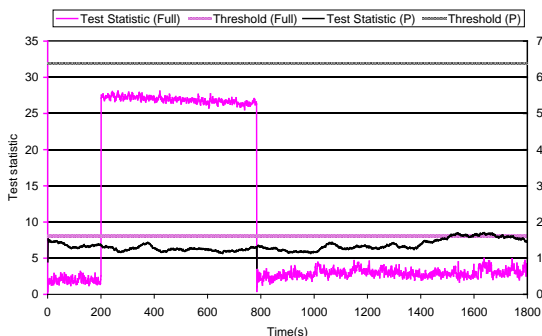


Fig. 5 Test statistics and thresholds for the of full set and the pseudorange subset

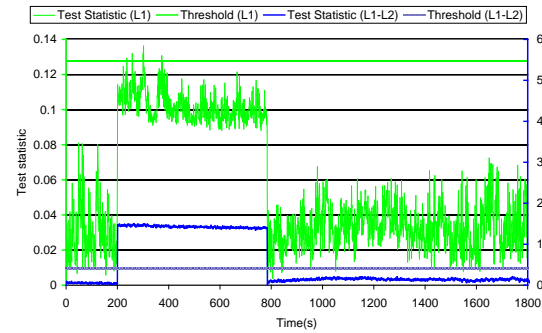


Fig. 6 Test statistics and thresholds for the wide-lane and L1 carrier subsets

The results show that the CRAIM algorithm proposed is able to detect the existence of the effect of cycle slips in L2 measurements in the cases of the full set and the wide-lane subset. However, a few detections occur in the L1 carrier and no detection occurs on the pseudorange subsets as they are not sensitive to the cycle slip(s) on L2. The cycle slip(s) disappears when the reference satellite changes since a new set of ambiguities are resolved at this time.

In the case of the protection level, the dominating factors are geometry and the covariance matrix. There is no significant difference in the protection level for the four scenarios. Figure 7 shows one example result of the protection level. The protection level is relatively stable except at the time (785th second) when the reference satellite changes followed by new ambiguities being resolved in a relative short time (within 2 seconds). This is where the peaks occur in the figure.

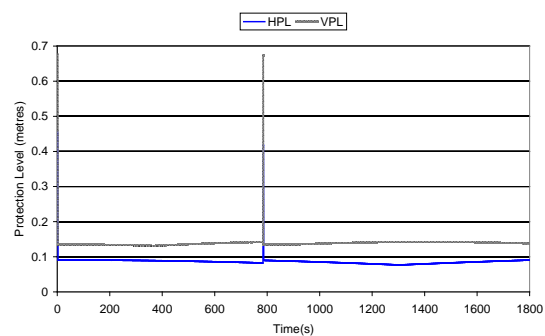


Fig. 7 Example result of protection level

3.3 Results of CRAIM for Integrated GPS/INS

The trial data injected with inertial sensor errors by simulating and adding step errors to the gyroscope and accelerometer data are used to demonstrate two scenarios below:

- Fault-free inertial sensor data
- A step error (1.0m/s^2) applied to the X accelerometer at the 45th second from the start of the trial

The position solutions using GPS carrier phase measurements together with the CRAIN algorithm are taken to represent the “true” (reference) trajectory for the analysis of the impact of inertial sensor failure on integrity monitoring. In order to show the results in horizontal and vertical components, the difference between solutions of different configurations is transformed/projected to an East-North-Up (ENU) coordinate representation. Figures 8 to 9 show the differences in positioning results determined from GPS only and integrated GPS/INS without INS failure. The differences in East and North are less than 1 cm in the static mode and less than 5 cm in the dynamic mode. The differences in Vertical (Up) are less than 2 cm. The relatively small differences justify the reasonability of the “truth” assumed above.

Figure 10 shows the test statistic plotted against the threshold. The test statistic is larger than the threshold in a few cases especially around the turning points A and B as shown in Figure 2. This shows the impact of dynamics on the integrity monitoring when inertial sensors are used. The inconsistency occurs not due to failure but due to the varying levels of sensitivity of the GPS receiver and inertial sensor to the dynamics of turning.

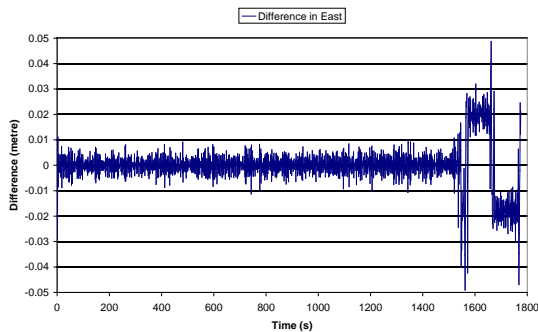


Fig. 8 Difference in East (no failure)

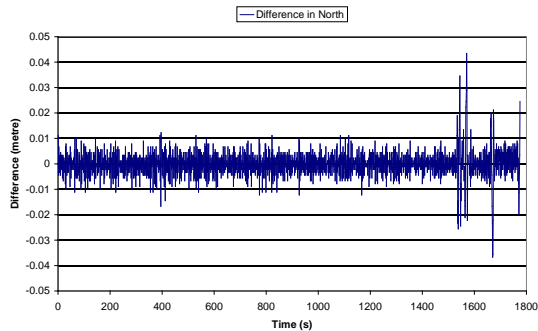


Fig. 9 Difference in North (no failure)

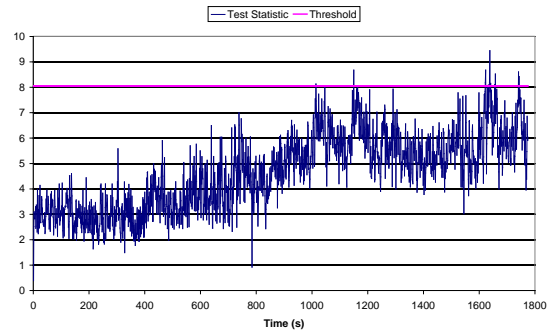


Fig. 10 Difference in Vertical (no failure)

Figures 11 to 12 show the differences in positioning results determined from GPS only and integrated GPS/INS with the X accelerometer being injected with a step error of 1m/s^2 . The differences in East and North at the start of the step are 0.25m and 1.1m respectively. The step error applied to the X accelerometer has a small impact on the difference in the vertical component at the point of introduction of the error. The differences converge to zero over time. This indicates that the Kalman filter is estimating and correcting the X accelerometer error. In the case of the dynamic mode, significant differences occur in all directions especially during changes in the azimuth and pitch. The change in pitch is due to the runway not being horizontal. Figure 13 shows the test statistic plotted against the threshold. The algorithm detects the step error immediately followed by a period of convergence after which the test statistic is less than threshold. However, when the car starts to manoeuvre, the test statistic exceeds the threshold, triggering failure detection.

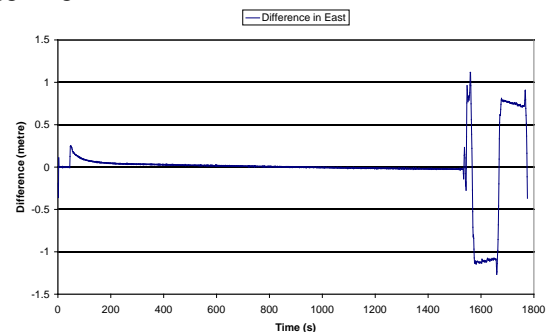


Fig. 11 Difference in East (accelerometer step error)

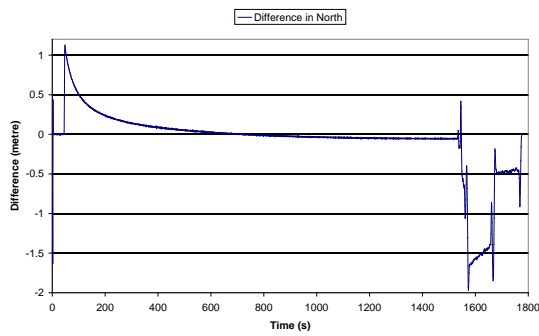


Fig. 12 Difference in North (accelerometer step error)

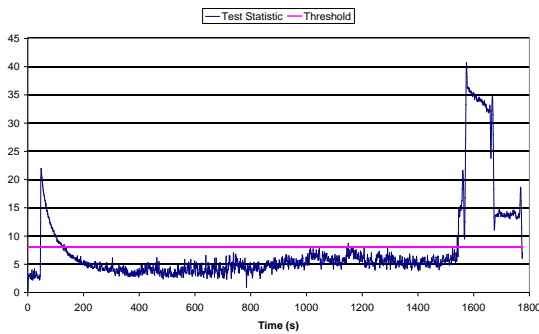


Fig. 13 Test statistic versus threshold (accelerometer step error)

3.4 Results of Group Separation

Simulation results are used below to demonstrate the method based on the assumption of a GPS satellite clock error modeling fault at the master control station which results in all satellites with a cesium clock having a ramp error of 0.05m/s. It should be noted that this example is used for illustration only. Future research will explore more realistic scenarios. The optimised constellation of 24 GPS satellites (RTCA/Do-229C, 2001) and the constellation of 27+3 Galileo satellites are used.

The ramp error is introduced to Cesium clocks starting at 3000 seconds of the week and ending at 6000 seconds of the week. Three satellites in view above a mask angle of 5 degrees are assigned this failure. The snapshot positioning algorithm is used ((Brown, 1996). Both the navigation system grouping and clock type grouping are used in the demonstration. Preliminary results using only pseudorange measurements are shown in Figures 14-16.

The test statistic versus threshold of the combined GPS and Galileo positioning is shown in Figure 14. The failure is detected at around 4300 seconds where the test statistic is larger than the threshold. Figures 3a and 3b show the test statistic versus threshold of the positioning results using the Galileo and GPS group separations respectively. In the GPS solution (Figure 15, where all Galileo measurements were excluded), the failure is detected almost at the same time (around 4300 second) as

in the combined solution. While in the Galileo solution (Figure 16), no failure is detected. Combining the results shown in Figures 14 and 16, the conclusion reached is that there is at least one failure in the GPS measurements. Hence, the Galileo measurements can be trusted for positioning. The results show that the group separation method has a reasonable level of efficiency.

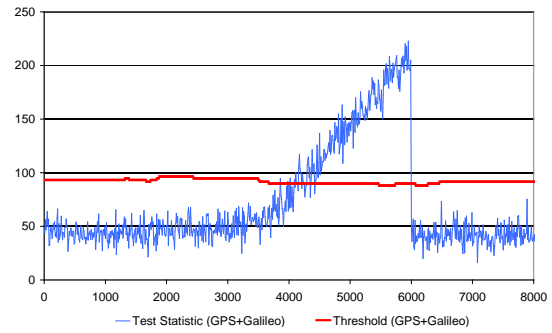


Fig. 14 Test statistic versus threshold for GPS+Galileo with 3 failures

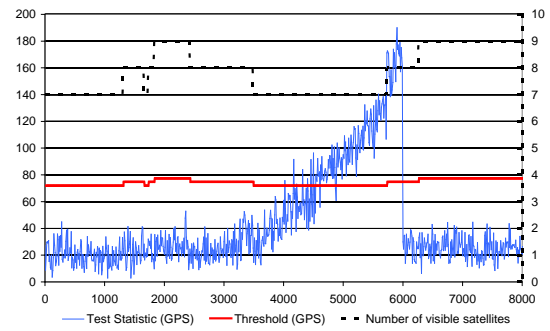


Fig. 15 Test statistic versus threshold for Galileo group separation (i.e. GPS only)

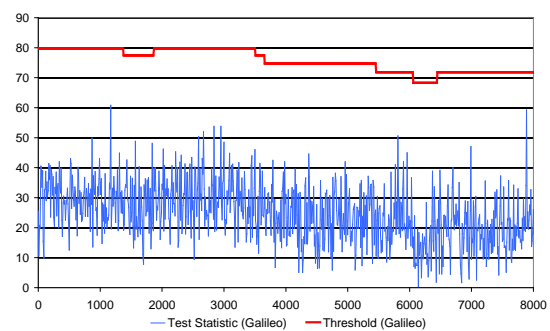


Fig. 16 Test statistic versus threshold for GPS group separation (i.e. Galileo only)

4. Conclusions

Carrier phased based integrity monitoring algorithms proposed in this paper successfully deal with the challenges identified and are able to monitor the accuracy at centimetre level. In particular, the new “difference

test" integrity monitoring algorithm can detect slowly growing errors significantly earlier than conventional algorithms. Furthermore, the algorithm based on group separation concept exploiting failure mode data can significantly reduce the computation load required for failure exclusion. The combination of the algorithms developed with existing ones, should provide reliable integrity monitoring and quality control for seamless positioning in all conditions and environments.

Acknowledgements

The research presented in this paper was supported by the SPACE project. SPACE (Seamless Positioning in All Conditions and Environments) was an EPSRC-funded collaborative research project and came to an end during 2008. It began life as a Pinpoint Faraday flagship project but, following the evolution of Pinpoint into a Knowledge Transfer Network (KTN), operates within the Location and Timing KTN (<http://www.locationktn.com>). It was undertaken by a consortium of eleven UK university and industrial groups. The university groups were the CAA Institute of Satellite Navigation at the University of Leeds, the Department of Civil and Environmental Engineering at Imperial College London, the Department of Geomatic Engineering at University College London (UCL), and the Institute of Engineering Surveying and Space Geodesy at University of Nottingham, and the industrial partners were The Civil Aviation Authority, EADS Astrium, Leica Geosystems, Nottingham Scientific Ltd, Ordnance Survey, QinetiQ and Thales Research and Technology.

The primary aim of SPACE was to undertake the basic research needed to build a prototype GNSS-based positioning system that can deliver cm-level accuracy positioning everywhere and at all times. The main component research thrusts were multipath modelling and mitigation, quality control and assessment, measurement modelling and integration, and GNSS sensor design. A key output from SPACE was a the fully tested design of a prototype plug and play integrated positioning system that can be used as a test bed for current and future positioning components and algorithms.

References

Brown, A., and Mathews, B. (2006): *A Robust GPS/INS Kinematic Integrity for Aircraft Landing*. Proceedings of ION GNSS, Fort Worth, TX, September 2006, pp715-725.

Brown, G. (1992): *A baseline GPS RAIM scheme and a note on the equivalence of three RAIM methods*. Navigation: The journal of the institute of navigation. Vol.39, No.3, Fall 1992, pp. 301-316.

Brown, R.G., Chin, Y.G. (1998): *GPS RAIM: calculation of thresholds and protection radius using Chi-Square methods-A geometric approach*. Global Positioning System: Papers Published in NAVIGATION. Volume V, 1998, 155-178.

Chang, X.W., Paige, C.C. and Perepetchai, V. (2001): *Integrity Methods Using Carrier Phase, Proceedings of International Symposium on Kinematic Systems in Geodesy*. Geomatics and Navigation (KIS 2001), Banff, Alberta, Canada June 5-8, 2001, pp. 235-245.

De Jonge, P., and Tiberius, C., (1996): *The LAMBDA method for integer ambiguity estimation: implementation aspects*. Tech Rep. 12, Delft Geodetic Computing Centre, IGR-series.

Diesel, J., and Luu, S., (1995): *GPS/IRS AIME: Calculation of thresholds and protection radius using Chi-square methods*. Proceedings of ION GPS 1995, Palm Springs, CA, 12-15, September 1995, pp1959-1964.

Ene, A., Blanch, J., Walter, T. (2006): *Galileo-GPS RAIM for Vertical Guidance*. Proceedings of ION NTM 2006, Monterey, CA, 18-20 January 2006.

Feng, S., Ochieng, W.Y. (2007a): *A Difference Test Method for Early Detection of Slowly Growing Errors in GNSS Positioning*. The Journal of Navigation 60(3) 2007, pp427-442.

Feng S, Ochieng WY., Hide, C., Moore, T. and Hill, C. (2007b): *Carrier Phase Based Integrity Monitoring Algorithms for Integrated GPS/INS Systems*. Proceedings of the European Navigation Conference, Geneva, Switzerland, 29-31, May, 2007.

Feng S, Ochieng WY (2006): *User Level Autonomous Integrity Monitoring for Seamless Positioning in All Conditions and Environments*. Proceedings of the European Navigation Conference, Manchester, 7-10, May, 2006.

Gold, K.L., Brown, A.K., (2004), *A Hybrid Integrity Solution for Precision Landing and Guidance*. Proceedings of IEEE PLANS, Monterey, CA, April 2004, pp165-174.

Hide, C., Moore, T. and Hill, C., (2006): *Development of a multi-sensor navigation filter for high accuracy positioning in all environments*. Proceedings of ION GNSS, Fort Worth, TX, September 2006, pp1635-1644.

- ICAO (2006): *Annex 10 Aeronautical Telecommunications, Volume I Radio Navigation Aids (Sixth Edition)*. 23/11/2006.
- Lee, Y. C. (2004): *Investigation of Extending Receiver Autonomous Integrity Monitoring (RAIM) to Combined Use of Galileo and Modernized GPS*. Proceedings of ION GNSS 2004, Long Beach, California, 21–24 September 2004.
- Lee, Y.C., O’Laughlin, D.G. (1999): *Performance analysis of a tightly coupled GPS/inertial system for two integrity monitoring methods*. Proceedings of ION GPS 1999, Nashville, Tennessee, 14-17, September 1999, pp.1187-1197.
- Michalson, W., Hua, H. (1995), *GPS carrier-phase RAIM*, Proceedings of ION GPS 95, Palm Springs, CA, September 1995, pp1975-1984.
- Offer, C.R., Grove, P.D., Macaulay, A.A. et al, (2006): *Use of Inertial Integration to Enhance Availability for Shipboard Relative GPS (SRGPS)*. Proceedings of ION GNSS, Fort Worth, TX, September 2006, pp726-736.
- Pervan, B., Lawrence D.G., and Parkinson, R.W., (1998): *Autonomous Fault Detection and Removal Using GPS Carrier Phase*. IEEE Transactions on Aerospace and Electronic Systems, 34(3), pp897-906.
- Pervan, B., Lawrence D.G., Cohen, C.E., and Parkinson, R.W., (1996): *Parity Space Methods for Autonomous Fault Detection and Exclusion Using GPS Carrier Phase*. Proceedings of IEEE PLANS, pp649-656.
- Pervan, B., Chan, F., et al, (2003): *Performance Analysis of Carrier Phase DGPS Navigation for Shipboard Landing of Aircraft*. Navigation: Journal of the Institute of Navigation, 50(3), pp181-191.
- RTCA/DO-229C (2001): *Minimum operational performance standards for global positioning system/ wide area augmentation system airborne equipment*. November, 2001.
- Teunissen, P.J.G., (2005): *Integer aperture bootstrapping: a new GNSS ambiguity estimator with controllable fail-rate*. Journal of Geodesy, Volume 79, Numbers 6-7, August 2005.